Sedimentation dynamics of spherical particles in confined geometries

E. Kuusela,[1] J. M. Lahtinen,[1] and T. Ala-Nissila[1,2]
[1]*Laboratory of Physics, Helsinki University of Technology, P.O. Box 1100, FIN-02015 Helsinki, Finland*
[2]*Department of Physics, P.O. Box 1843, Brown University, Providence, Rhode Island 02912–1843, USA*
(Received 25 June 2003; revised manuscript received 2 March 2004; published 16 June 2004)

We study the steady-state dynamics of sedimenting non-Brownian particles in confined geometries with full hydrodynamic interactions at small but finite Reynolds numbers. We employ extensive computer simulations using a method where a continuum liquid phase is coupled through Stokesian friction to a discrete particle phase. In particular, we consider a sedimentation box which is otherwise periodic except that it is confined by two parallel walls parallel to gravity with a spacing L_x. By systematically varying L_x we explore the change in dynamics from a quasi-two-dimensional (2D) case to a three-dimensional case. We find that in such confined geometries there is a depletion of particle number density at the walls for small volume fractions, while for large volume fractions there is an excess number of particles at the walls. For the average sedimentation velocity, we find that the Richardson-Zaki law is well obeyed but the decrease of the velocity for dilute systems is slower for smaller values of L_x. We study the anisotropy of the velocity fluctuations and find that in the direction of gravity there is excellent agreement with the predicted scaling with respect to L_x. We also find that the behavior of the corresponding diffusion coefficients as a function of L_x is qualitatively different in the direction parallel to gravity and perpendicular to it. In the quasi-2D limit where particles block each other, the velocity fluctuations behave differently from the other confined systems.

DOI: 10.1103/PhysRevE.69.066310 PACS number(s): 47.55.Kf, 05.40.−a, 68.35.Fx, 82.70.−y

I. INTRODUCTION

The transport properties of sedimenting particles play an important role in many natural processes and industrial applications. This problem is also an interesting example of nonequilibrium dynamics, which is still somewhat poorly understood in the case of a finite volume fraction Φ of the particles [1]. Under appropriate boundary conditions, such as in fluidized beds, a sedimenting system driven by gravity can reach a steady-state distribution, with a fixed average settling velocity $V(\Phi) \equiv |\langle \mathbf{V} \rangle|$, where $\mathbf{V} = (1/N)\Sigma_{i=1}^{N} \mathbf{v}^i$ is the average velocity of N sedimenting particles and the angular brackets denote a *steady-state* average. An important special case of sedimentation is that where experiments have been carried out in systems with confined geometries, in particular in between closely spaced glass plates where even a quasi-two-dimensional (2D) geometry can be realized [2,3]. One of the benefits of such a setup is that it is possible to visually determine the position and velocity of each individual particle. However, it is not presently clear how the measurements in such a system can be quantitatively related to the corresponding values measured in true 3D experiments or simulations. For example, it is expected that closely placed walls influence the behavior of the sedimenting particles by restricting the particle motion due to enhanced blocking and, on the other hand, due to the effect of the friction produced by the no-slip boundary conditions along the walls. Also, the role of inertial effects is an open question.

In a 3D system the behavior of $V(\Phi)$ has been extensively studied in the limit where Brownian motion can be neglected [4–10]. Both experiments and simulations have shown that as Φ increases $V(\Phi)$ decreases monotonically following the phenomenological Richardson-Zaki (RZ) law

$$V(\Phi)/V_s = (1-\Phi)^n, \tag{1}$$

where V_s denotes the terminal settling velocity (Stokes velocity) of a single particle and the exponent n is around 4.5–5.5 in the low Reynolds number (Re) regime [11]. Qualitatively the monotonically decreasing behavior can be understood as the increasing effect of the backflow. In the low Re and Φ limit Batchelor [7] deduced the result $V(\Phi)/V_s = 1 - 6.55\Phi$ for the case where the system size $L \to \infty$. To obtain this result, it was assumed that particles cannot overlap but otherwise all configurations are equally probable. Similarly, Geigenmüller and Mazur [12] (and later Bruneau *et al.* [13,14]) studied the effect of the side walls on the sedimentation velocity. Assuming that particles do not overlap with walls, an *intrinsic convection* flow is formed in the vicinity of the walls due to depletion of particles in a distance closer to the wall than the particle radius. In the special case where the suspension is confined between two infinite parallel vertical walls, this convection leads to an average settling velocity that is a function of the position relative to the walls. Finally, we note that in the 2D limit, where only few studies exist, the RZ law is well obeyed but with an effective exponent $n \approx 3$ [10].

During sedimentation each particle produces a velocity field around it which, in the creeping flow limit, decays as r^{-1} where r is the distance from the particle center. This velocity field influences the motion of the other particles [15]. With random fluctuations in the particle density this hydrodynamic interaction induces, even without Brownian motion, fluctuations around the average velocity $V(\Phi)$ for $\Phi > 0$, which leads to *diffusive* behavior of the particles. In the direction of gravity (negative z axis here), the fluctuations are defined by

$$\Delta V_z = \sqrt{\langle \delta v_z^2 \rangle}, \tag{2}$$

where $\delta v_z = v_z + V(\Phi)$ is the one-particle velocity fluctuation where the ballistic average motion has been removed from the velocity component parallel to gravity. The nature and origin of these velocity fluctuations have been under intense experimental and theoretical studies recently [1]. Of particular interest is the dependence of the velocity fluctuations ΔV on Φ and on the dimensions of the container. Early theoretical work concerning 3D systems by Caflisch and Luke [16] predicted that in the limit where inertial effects are negligible, the velocity fluctuations would diverge with the system size as $\Delta V/V_s \sim \Phi^{1/2}(L/a)^{1/2}$, where L is the linear size of the container and a is the particle radius. An intuitive way to obtain this result is to consider that a "blob" of N_{ex} excess particles in a volume of linear dimension ρ is sedimenting with relative velocity $V_s N_{\mathrm{ex}} a/\rho$. If the particle distribution is uniformly random, it can be assumed that there exists a blob with $\rho \sim L$ and $N_{\mathrm{ex}} \sim \sqrt{L^3 \Phi}$ producing velocity fluctuations with the given scaling [17,38].

Such divergence has been observed in numerical simulations of Ladd performed in periodic systems [9,18]. However, in experiments it has been observed that the velocity fluctuations saturate at a certain system size beyond which the container does not have any effect [6,19]. In particular, Nicolai and Guazzelli used containers whose width varied from $51a$ to $203a$ and found no systematic increase in the velocity fluctuations [19]. Such results indicate that the size of the region where the particle motion is correlated is somehow reduced to a volume that is not proportional to the size of the container. This has also been observed directly by measuring the spatial velocity correlation length from the sedimenting suspension [6]. This has been recently shown to be the result of the horizontal walls of the container: there is a particle number density gradient which reduces the spatial size of the particle density fluctuations even if the spacing of the side wall diverges [20–22].

Furthermore, Koch and Shaqfeh [23] have shown that if, instead of a uniformly random particle distribution, there is a sufficient average net depletion of other particles around each particle that also leads to saturating velocity fluctuations. Later Koch [24] showed that if $\mathrm{Re} \approx \mathcal{O}(1)$, the wake behind the particle will suffer such a depletion leading to $\Delta V^2 \sim \mathcal{O}\{\Phi V_s^2[\ln(1/\Phi) + \mathrm{const}]\}$.

An interesting special case is an unisotropic rectangular container. According to Brenner [26], if the walls exert no force on the fluid, it is the largest dimension which controls the behavior of ΔV. However, if no-slip boundary conditions are used, the smallest dimension restricts the growth of the fluctuations. Brenner studied a system that was confined between two vertical walls and noted that depending on Φ and the spacing of the walls L, the sedimenting particles could either be interacting strongly with the r^{-1} interaction or weakly, with an interaction decaying faster. This was based on the results of Liron and Mochon [27], who calculated that due to the particle-wall interaction, the velocity field around each particle decays as r^{-2} or faster whenever $r \gg d$, where d is the distance to the closest wall. If Φ and L are sufficiently small, the particles are typically closer to the walls than to each other and the system is said to be weakly interacting [26]. On the other hand, increasing Φ or L will eventually lead to a system where the particles are closer to each other than to the walls and the system is strongly interacting. Brenner also assumed that in a weakly interacting system, the particles are spaced uniformly but in a strongly interacting system they are depleted from the center of the container since the particle diffusion is largest there due to the larger velocity fluctuations.

In simulations, periodic boundary conditions are often used. Even though no walls are present, additional force is exerted on the fluid by the periodic images. The contribution from the periodic images hinders the fluid velocity produced by the particle motion. Koch showed that in a geometry, where the height of the container is much larger than the other two equal dimensions, the velocity fluctuations are controlled by the smaller dimension [25]. Similar results were also obtained by Ladd using a lattice Boltzmann simulation technique [18].

Another important quantity which is affected by size effects of the container is the single particle (tracer) diffusion coefficient D defined by the Green-Kubo relation [28]

$$D = \frac{1}{d}\int_0^\infty C(t)dt, \tag{3}$$

where d is the spatial dimension and $C(t)$ is the particle velocity *fluctuation* autocorrelation function

$$C(t) \equiv \langle \delta \mathbf{v}(t) \cdot \delta \mathbf{v}(0) \rangle. \tag{4}$$

Since $C(0) = \Delta V^2$, Eq. (3) is often written in the form $D = d^{-1}\Delta V^2 \tau$ where τ is the velocity autocorrelation time. It has been found in analytical work [25] and simulations [9] that also τ depends on the system size. In experiments the measured values of τ have been found to saturate in large systems [19].

In this work we present comprehensive numerical results on the behavior of velocities, their fluctuations and the tracer diffusion coefficients of non-Brownian spheres with a finite Reynolds number in a system, where periodic boundaries are used in the direction parallel to the gravity (z) and one direction perpendicular to it (y), but in the third direction (x) the suspension is confined between two walls with no-slip boundary conditions (Fig. 1). While the separation of the walls increases the system changes from a quasi-2D setup to a 3D container. We study the influence of the wall friction and the change in the spatial degrees of freedom here, when crossing over from the quasi-2D limit to 3D. The periodic boundaries in the direction of gravity make it possible to obtain a steady-state condition here, and thus also the velocity fluctuations do not saturate in this direction. Due to the use of a highly asymmetric simulation box, we expect that the behavior of the velocity fluctuations and diffusion coefficients are highly anisotropic.

II. MODEL

We use an immersed boundary method developed by Schwarzer and Höfler [29] to model a 3D suspension of non-

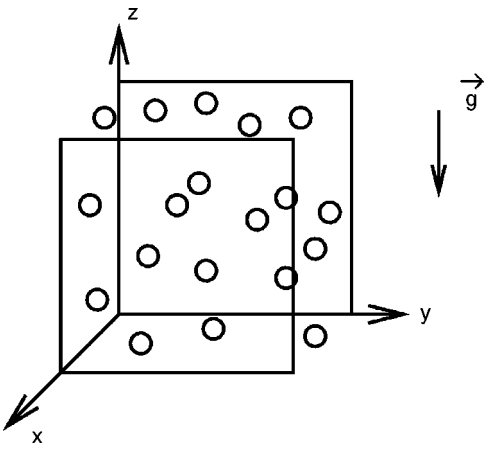

FIG. 1. A schematic figure of the geometry of the sedimentation box. The direction of gravity is along the negative z axis, with periodic boundary conditions in both the z and y directions. The confining walls with a variable spacing L_x are placed in the x direction.

Brownian particles with a *particle* Reynolds number of $\mathrm{Re}_p = V_s \rho_l a / \eta = 0.5$, where ρ_l is the density of the fluid and η the viscosity of the fluid. The model is based on continuum description of an incompressible Newtonian fluid and uses a finite-difference method on a regular grid to find a pressure p and a velocity field $\mathbf{u}$ of the fluid that would simultaneously satisfy the equation of continuity

$$\nabla \cdot \mathbf{u} = 0, \tag{5}$$

and the Navier-Stokes equation [30]

$$\frac{\partial \mathbf{u}}{\partial t} + (\mathbf{u} \cdot \nabla)\mathbf{u} = -\rho_l^{-1} \nabla p + \frac{\eta}{\rho_l} \nabla^2 \mathbf{u} + \mathbf{f}. \tag{6}$$

The additional force density field $\mathbf{f}$ contains the effect of gravity and also a fictitious term to ensure that in the interior of the domain of the particles $\mathbf{u}$ coincides with the motion of a rigid body. This force is derived by tracking explicitly the motion of the solid particles and whenever the motion of the fluid and the particle templates differ in certain predefined points, a restoring force is added. The method is suitable for modeling non-Brownian suspensions up to $\mathrm{Re}_p \approx 10$, and has been tested for a variety of different cases. More details can be found in Ref. [29].

In the simulations the units have been chosen so that the radius of the particles, the density of the fluid, and the Stokes velocity are all equal to unity. In this unit system time is measured in terms of the Stokes time, i.e., the time it takes a particle with velocity V_s to travel a distance of one radius. In all our simulations here the density of the particles is 2.5 times the density of the fluid. The lattice spacing of the discretization of the fluid velocity and pressure field is 0.335, and 81 markers per particle are used to model the coupling between the fluid and the particles. Periodic boundaries used in the direction of gravity ensure that the steady state is reached, which takes typically several hundred Stokes times. For the periodic dimensions $L_y = L_z = L_{\mathrm{periodic}}$ we use values 22.76, 45.51, and 91.02, while the separation of the walls in the confining x direction L_x varies between 3.2 and 45.87 particle radii. The smallest separation was chosen such that particles truly block each other when moving downward and thus the geometry is quasi two dimensional. The volume fraction in a simulation is given by $\Phi = 3(L^2_{\mathrm{periodic}} L_x)/(4\pi N)$. The number of particles varies from 10 to 4536. It is important to note that since the Stokes velocity V_s is defined as the terminal velocity of a single particle with a unit radius in an infinite container, the terminal velocity of a single sphere in a finite container V_0 differs from V_s and depends on the container dimensions [31,32].

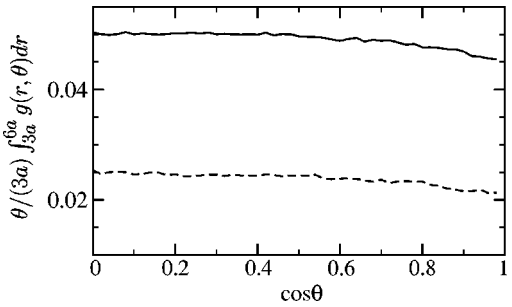

FIG. 2. The θ dependence of the pair correlation function. See text for details.

III. RESULTS

We will first study the particle density distributions relative to a test particle and in the direction between the walls. We will analyze the average settling velocity and the average velocity distribution between the walls. Then we will discuss the spatial velocity correlations and analyze the velocity fluctuations. Finally we show results for the corresponding diffusion coefficients.

A. Particle density distribution

We start by considering the particle density distribution. The pair distribution function

$$g(\mathbf{r}) = \left\langle \frac{1}{N} \sum_{j \neq i} \delta(\mathbf{r} - (\mathbf{r}^i - \mathbf{r}^j)) \right\rangle \tag{7}$$

is computed to find out whether the approximation of uniform distribution is valid or not. Here $\mathbf{r}^i$ and $\mathbf{r}^j$ denote the position of the particles i and j. We found that there is a region of smaller particle density above each particle, and due to symmetry of $g(\mathbf{r})$ below as well, as described by Koch [24]. We have demonstrated this qualitative agreement in Fig. 2, where we have plotted $\Phi/(3a)\int_{3a}^{6a} g(r,\theta)dr$ as a function of $\cos\theta$, where θ is the angle between $\mathbf{r}$ and the direction of gravity. The data are presented from fully periodic simulations with dimensions $32 \times 64 \times 32$ and for volume fractions $\Phi = 0.025$ (dashed line) and 0.05 (solid line).

In Fig. 3 we present the particle number density distribution function

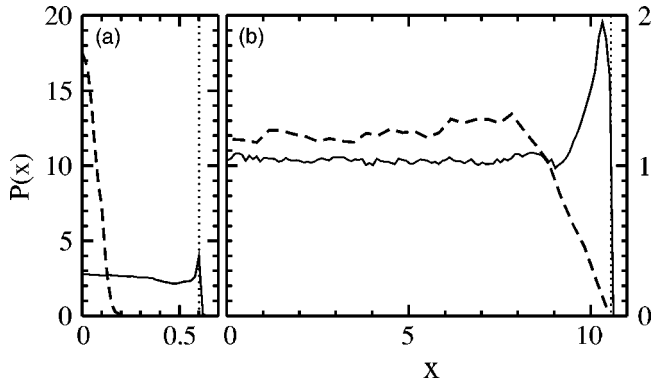

FIG. 3. Normalized particle number density as a function of the x coordinate measured from the middle of the system: (a) wall spacing $L_x=3.2$, $\Phi=0.025$ (dashed line), $\Phi=0.225$ (solid line). (b) $L_x=23.11$, $\Phi=0.025$ (dashed line), $\Phi=0.152$ (solid line). The vertical dotted line marks the distance of one-particle radius away from the wall. Note the difference in the vertical scales between (a) and (b).

$$P(x)=\left\langle \frac{L_x}{N}\sum_{i=1}^{N}\delta(x-x^i)\right\rangle \tag{8}$$

between the walls with two different values of L_x and Φ. Here x^i denotes the x coordinate of particle i measured from the middle of the system. The data are normalized such that particle density $P(x)=1$ corresponds to a particle density in an infinite system with a spatially uniform distribution with the same volume fraction. In both quasi-2D [Fig. 3(a)] and $L_x=23.11$ cases (b) the particles in a dense suspension are distributed quite evenly except for an excess density next to the wall. The vertical dotted line represents the value of x where the particle touches the wall. With wall spacing $L_x=23.11$ the shape of $P(x)$ in the vicinity of the wall closely follows the particle-wall correlation function obtained by assuming a random particle configuration except for a hard-sphere potential between the particles and a similar particle-wall interaction, as calculated by Bruneau *et al.* [14]. Peysson and Guazzelli have found a similar distribution in their non-Brownian sedimentation experiments, where $\mathrm{Re}_p<0.001$ [33].

As shown for $\Phi=0.025$ [dashed line in Fig. 3(a)], in the dilute limit $P(x)$ differs from both the experiments of Peysson and Guazzelli and the theoretical distribution of a uniformly random configuration of hard spheres, in which case the low particle density limit of $P(x)$ should be close to a step function with a zero value if $x>L_x/2-a$ and a constant otherwise. Instead there is a distinct depletion layer which extends several particle radii away from the wall. In the case of small L_x, all the particles are concentrated close to the center of the container. Due to the wider, and Φ dependent, depletion layer it is convenient to define an *effective width* $L_x^{eff}=4\int_0^{L_x/2}P(x)x\,dx$. With this, the width of the depletion layer is defined as $\zeta_x=1/2(L_x-L_x^{eff})$. As can be seen from Fig. 4, when Re_p is kept constant, ζ_x is only a function of Φ, provided that the width of the system is large enough. Furthermore there seems to be a power-law scaling $\zeta_x\sim\Phi^{-m}$, with the fitted exponent $m\approx0.60$.

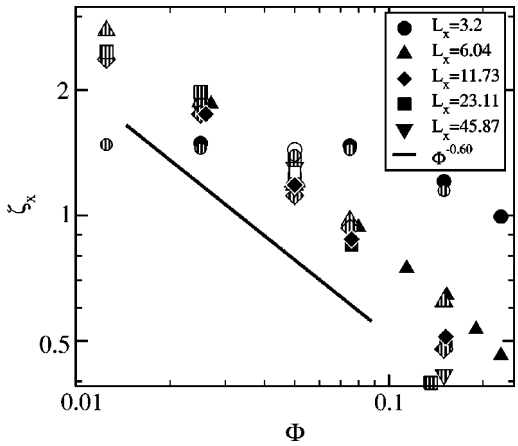

FIG. 4. The width of depletion layer as function of the volume fraction Φ. The data for $L_{\mathrm{periodic}}=22.76$, 45.51, and 91.02 are presented using solid, striped, and open symbols, respectively. The solid line presents $\zeta_x\sim\Phi^{-0.60}$. Note that in the quasi-2d limit, ζ_x is almost independent of Φ since the particles are concentrated in the middle of the system. Error bars in this and the following figures are smaller or equal to the size of the symbols when not explicitly shown.

This discrepancy with the experimental results in low Re_p is a direct consequence of the inertial effects. Although a systematic study of the effect of Re_p is beyond the scope of this paper, we did additional studies with $\mathrm{Re}_p\neq0.5$ and found that $P(x)$, and ζ_x strongly depend on Re_p. For example, in the case of $L_{\mathrm{periodic}}=45.511$, $L_x=6.044$, and $\Phi=0.05$ we found that ζ_x increases from 0.95 to 1.43 when Re_p changes from 0.1 to 1. This behavior is reasonable since in a region of finite Re_p particle sedimenting between two infinite vertical walls is shown by Vasseur and Cox [34] to migrate away from the closer wall due to a repulsive particle-wall interaction. On the other hand, as discussed in the analysis of moderate Re_p by Koch [24], the particle migrates away from the wake of another particle. It would thus be reasonable to assume that the depletion regime of the steady-state distribution $P(x)$ presents a situation where the particles interact with the wall and the other particles with equal strength. Furthermore with moderate Re_p a particle induces r^{-1} flow only to its wake whose width is proportional to the square root of the distance from the particle center, suggesting that $\zeta_x\sim\Phi^{-1/2}$.

B. Average sedimentation velocity

The intrinsic convection produced by the nonuniform $P(x)$ is seen in

$$V(x)=\left\langle \sum_{i=1}^{N}v_z^i\delta(x-x^i)\right\rangle \Bigg/ \left\langle \sum_{i=1}^{N}\delta(x-x^i)\right\rangle \tag{9}$$

shown in Fig. 5 for the same two system widths and volume fractions as in Fig. 3. Even though the average volume flow across horizontal cross section is set to zero, a convection is

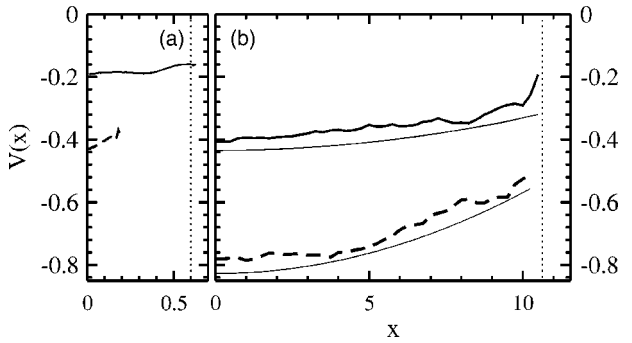

FIG. 5. Average particle settling velocity as function of the x coordinate measured from the middle of the system: (a) wall spacing $L_x=3.2$, $\Phi=0.025$ (dashed line), $\Phi=0.225$ (solid line). (b) $L_x=23.11$, $\Phi=0.025$ (dashed line), $\Phi=0.152$ (solid line). The vertical dotted line marks the distance of one-particle radius away from the wall. The two thin solid lines in (b) are parabolic fits to the data (shifted for clarity).

induced to the system: in the depletion regime close to the wall the fluid is moving upwards and there is correspondingly a downward net flow in the center region of the container. In the central region of the system with $L_x=23.11$ the velocity profile closely follows a parabola. There is a qualitative agreement to the theoretical predictions obtained by assuming $P(x)$ to be a step function [12] or a random configuration of hard spheres [14].

In Fig. 6 we show the normalized settling velocity $V(\Phi)/V_s$ averaged over x for different values of L_x. The first data points at $\Phi=0$ correspond to the size-dependent one-particle velocity V_0 measured when the particle sediments in the middle of the system. The data are well approximated by the expression

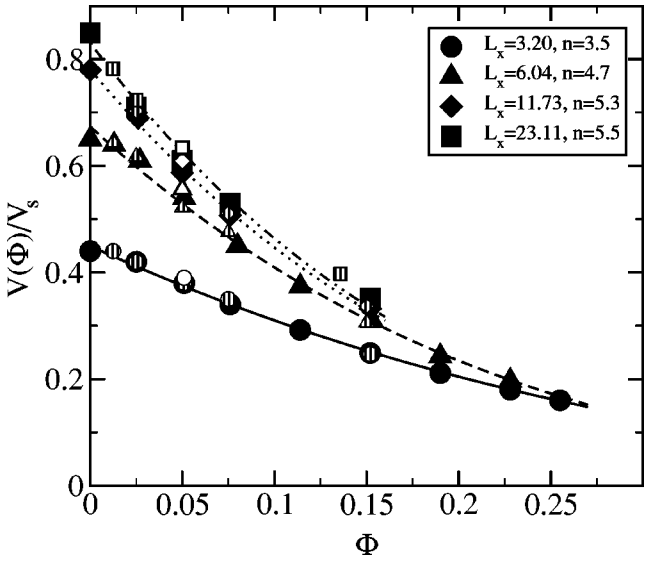

FIG. 6. The normalized average settling velocity $V(\Phi)/V_s$ for different wall spacings L_x. The lines are fits to the data. The data for $L_{\text{periodic}}=22.76$, 45.51, and 91.02 are presented using solid, striped, and open symbols, respectively.

$$V_0 \approx [1-0.502(a/L_x)+0.0523(a/L_x)^3+0.0131(a/L_x)^4 - 0.005(a/L_x)^5]V_s \tag{10}$$

which has been derived for a sphere in the middle of a system between two parallel, infinite walls, with $\mathrm{Re}_p=0$ [32]. Our values are consistently slightly less than those predicted by Eq. (10) due to the finite Re_p effects [32] and the periodic boundaries in the y and the z directions [31]. As expected, with all the values of L_x here the average settling velocity is a monotonically decreasing function of the volume fraction Φ. All the data can be well fitted with the RZ law, but the exponent of the power law n depends on L_x. In the widest (3D) geometry the exponent is found to be 5.5 in good agreement with 3D experiments [19]. On the other hand, for the most narrow case where particle blocking is in effect, $n=3.5$ which indicates a considerably slower decay in accordance with the previous studies [10,36].

However, our results show that since in Fig. 6 the normalization factor V_s is that of an infinite 3D system, the effect of the wall spacing rapidly decreases as a function of Φ, and even for the quasi-2D case it becomes negligible beyond $\Phi \approx 0.2$. The effect of the walls is weakened by both the intrinsic convection, and also by the fact that with larger Φ a smaller portion of the particles are strongly interacting with the walls.

C. Velocity fluctuations

Unlike the average settling velocity, the behavior of the velocity fluctuations is expected to be much more sensitive to changes in the size of the container, due to the dependence of the spatial correlation length of the velocities. Before discussing the velocity fluctuations we study the spatial velocity correlation (SVC) function of the particles defined as

$$R_{\alpha\beta}(r)=\frac{\langle v_\alpha^i v_\alpha^j\rangle_\beta(r)-\langle v_\alpha^i\rangle_\beta^2(r)}{\langle (v_\alpha^i)^2\rangle_\beta(r)-\langle v_\alpha^i\rangle_\beta^2(r)}, \tag{11}$$

where α and β can denote any of the spatial directions x, y, or z while v_α^i and v_α^j are the α component of the velocity of particles i and j. With $\langle\cdot\rangle_\beta(r)$ we denote a steady-state average over all pairs whose orientation differs less than 5 degrees from the direction of β and have a spatial distance of r. Excluding R_{zz}, none of the spatial velocity correlations depends strongly on Φ. Instead they seem to scale according to the dimensions of the container indicating that the current simulations are not in the same limit than the sedimentation experiments of Segré *et al.* [6] where the SVC correlation lengths saturated to values that depend only on Φ. Since the saturation value was about 20 $a\Phi^{-1/3}$ it is reasonable to assume that no saturation happens in our $L_{\text{periodic}}\leqslant 91.02$ containers. A further reason not to expect similar scaling in the present simulations is that the saturation has been shown to be a result of having walls in the direction of gravity. However, the experiments of Bernard-Michel *et al.* [35], performed in a long tube with smaller square cross section (width less or equal than $800a$) show almost linear relation between the correlation length of the SVC and the width of the container with no Φ dependence.

In all directions our measured $R_{x\beta}(r)$ depends only on L_x provided that $L_x < L_{\text{periodic}}$. The correlation lengths are, however, different in each direction being smallest in the z direction, and largest in the y direction. The shapes of $R_{xx}(r)$ and $R_{xz}(r)$ are quite similar to the corresponding SVC's shown in Ref. [35]. For the y component of the particle velocities all correlation lengths increase seemingly linearly with increasing L_{periodic}. In addition, there is also a much weaker, and unsystematic increase of the correlation length with increasing L_x, most notably in the x direction. We performed some simulations with a container where $L_y \neq L_z$ which seem to suggest that in such cases the correlation lengths of $R_{yy}(r)$ and $R_{yz}(r)$ are defined by the smaller of these dimensions, which is again in a good agreement with the results in Ref. [35]. The correlation lengths of $R_{zx}(r)$ and $R_{zy}(r)$ seem to depend both on L_x and L_{periodic} even when the former is much smaller than the latter. This time simulations performed with $L_y \neq L_z$ indicate that the correlation lengths depend on L_y even if $L_y < L_z$ leading again to a scaling similar to that in Ref. [35]. The scaling of $R_{zz}(r)$, however, differs significantly from the previous by the fact that the correlation length depends also on Φ. With increasing Φ the correlation length decreases systematically in all cases studied, except in the system with $L_x \leqslant 6.044$ and $L_{\text{periodic}} = 22.76$ where the correlation length depends on the volume fraction only if $\Phi \geqslant 0.08$. This result can be understood as a direct consequence of the depletion region above the test particle and is thus a finite Re_p phenomenon. The simulations with $L_y \neq L_z$ seem to indicate that in the case of $R_{zz}(r)$ the correlation length depends more strongly on the ratio L_y/L_z than L_{periodic} in the case when $L_y = L_z$.

In Figs. 7(a), 8(a), and 9 we present the normalized velocity fluctuations $\Delta V(\Phi)/V_s$ in the z, x, and y directions, respectively. In each figure we have presented the data obtained by using different L_{periodic} and three different lengths in the periodic dimensions: 22.76, 45.51, 91.02, presented by solid, striped, and open symbols respectively. First, it can be seen that the qualitative behavior as a function of the volume fraction Φ is the same in all directions and with all values of L_x, except in the quasi-2D limit in the x direction, namely, the fluctuations increase initially with Φ due to the increasing effective particle interactions, but for larger values of Φ mutual blocking effects render $\Delta V/V_s$ a decreasing function of Φ as seen in numerous previous experiments [37,38]. The absolute values of the velocity fluctuations are quite close to those obtained by Ladd using lattice Boltzmann simulation technique with periodic boundaries in all directions [9,18]. With increasing system size the velocity fluctuations obtained by Ladd, however, increase faster than our results. Likewise, in the z direction with $\Phi = 0.05$ the absolute values of the velocity fluctuations are of the same order of magnitude as in the experiments of Nicolai and Guazzelli [19], which were performed in containers that have a width of 51 particle radii, or larger, and other dimensions much larger than the systems studied here.

In the direction parallel to gravity the size of the velocity fluctuations depends strongly on L_x and only weakly on the other dimensions, especially when the container aspect ratio L_x/L_{periodic} is small. The finite-size scaling follows $\Delta V_z/V_s \sim L_x^{1/3}$ with good accuracy, except in the quasi-2D limit, as shown in the inset of Fig. 7(b). This is in an apparent contradiction with the prediction of Caflisch and Luke [16] that $\Delta V_z/V_s \sim L^{1/2}$. The weak but systematic increase of the scaled velocity fluctuations with increasing L_{periodic} suggests that systems with the same ratio L_x/L_{periodic} could have a somewhat different scaling. We found that when comparing the pairs of systems with approximately the same L_x/L_{periodic}, the increase of velocity fluctuations with the increasing container size does not contradict the prediction of Caflisch and Luke [16] provided that $L_x/L_{\text{periodic}} > 1/8$. The quasi-2D limit is also different from the rest of the data in that it does not obey the finite-size scaling law, with values about 40% less than expected from the $L_x^{1/3}$ scaling.

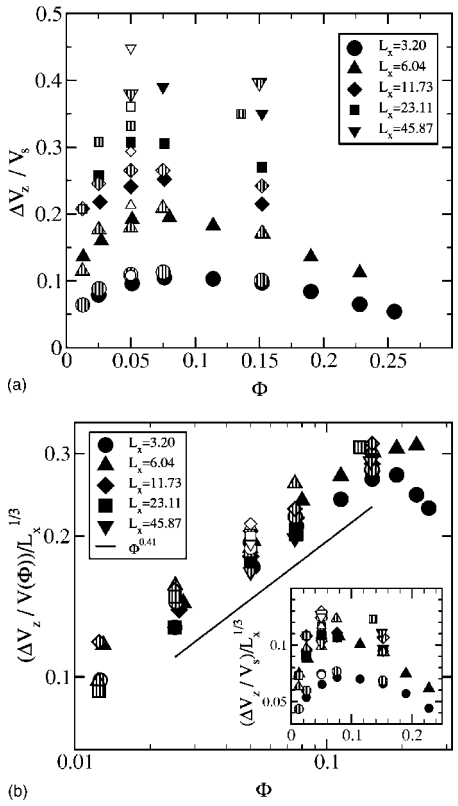

FIG. 7. Velocity fluctuations in the z direction parallel to gravity. In Figs. 7–9, the solid, striped, and open symbols denote $L_{\text{periodic}} = 22.76$, 45.51, and 91.02, respectively.

In order to find out the Φ and L_x scaling of ΔV_z, it is necessary to normalize the velocity fluctuations with $V(\Phi)$ rather than V_s [6,35]. In the main plot of Fig. 7(b) we show $\Delta V_z/V(\Phi) \sim L_x^{1/3}$. We find that in dilute systems, these fluctuations obey a power law $\Delta V_z/V \sim \Phi^{\xi}$, with $\xi = 0.41 \pm 0.01$ instead of $\xi = 1/2$ as predicted by Caflisch and Luke [16]. The weaker scaling may be an effect of the Φ dependence in the correlation length of $R_{zz}(r)$. This value of ξ is, however, very close to what has been seen in the experiments [6,22,35] even though some of these systems are thought to have different kind of scaling due to the volume fraction gradient which is not present in our system. Also in agreement with experiments [38], $\Delta V_z/V$ does not follow a power law behavior for larger volume fractions.

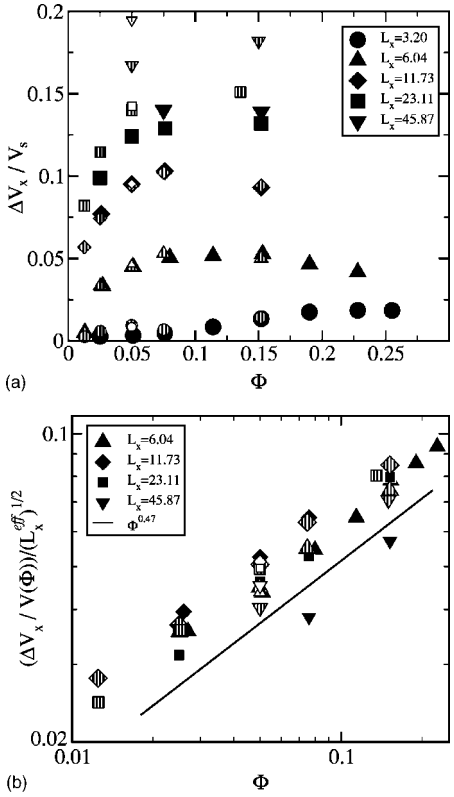

FIG. 8. Velocity fluctuations in the x direction perpendicular to the walls.

Quite similar to the fluctuations in the direction of gravity, ΔV_x does not scale at all with the periodic dimensions, provided that L_x is smaller than the other dimensions. Such a result is reasonable since the correlation length of the x component of the particle velocities depends only on L_x. The scaling with the wall spacing is, however, somewhat different. Instead of L_x scaling, we find that $\Delta V_x/V$ scales reasonably well with L_x^{eff}. In Fig. 8(b), in which normalization with $V(\Phi)$ rather than with V_s was used, we show that $\Delta V_x/V(\Phi)/(L_x^{eff})^{1/2}$ scales as Φ^{ξ} with $\xi=0.47\pm0.03$. Since the scaling exponent of Φ and L_x^{eff} is essentially the same this

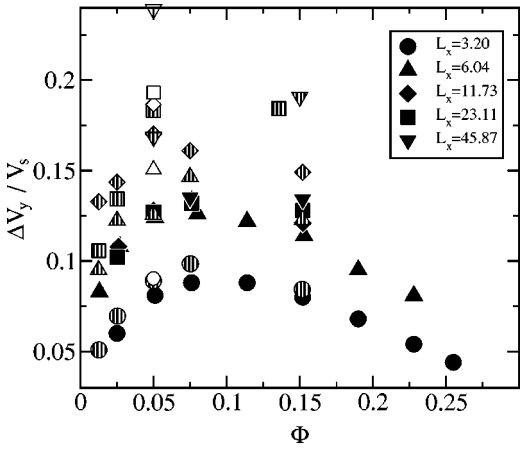

FIG. 9. Velocity fluctuations in the horizontal y direction parallel to the walls.

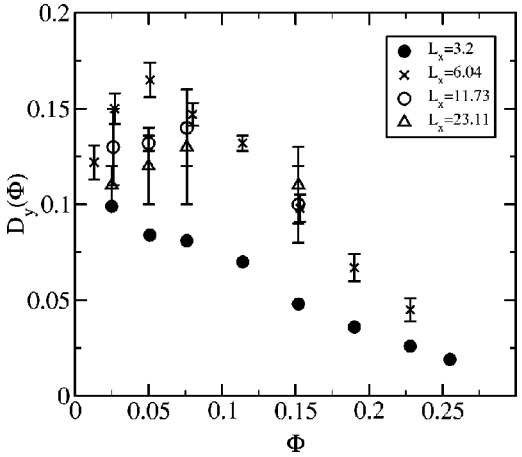

FIG. 10. The tracer diffusion coefficient in the horizontal y direction parallel to the walls.

can be interpreted as $L_x^{1/2}(\Phi^{eff})^{1/2}$, where $\Phi^{eff}=\Phi L_x^{eff}/L_x$ is the average volume fraction in the volume occupied by the particles. Again, by only considering containers with approximately the same aspect ratio we note that with fixed L_x/L_{periodic} the scaling of $\Delta V_x/V_s$ does not contradict the predictions of Caflisch and Luke [16] provided that $L_x/L_{\text{periodic}}>1/4$.

The behavior of $\Delta V_y/V_s$ in the periodic y direction is less clear as shown in Fig. 9. We were not able to find any clear scaling law. It seems, however, that in a dilute suspension the wall spacing limits the velocity fluctuations only if $L_x/L_{\text{periodic}}\lesssim 1/4$. At this point ΔV_y has values of the same order as ΔV_x in a container with equal dimensions and any further increase of L_x does not affect these values significantly. In a more dense suspension with $\Phi=0.15$ there is a systematic increase of ΔV_x with increasing L_x.

Finally, we note that the ratio $\Delta V_z/\Delta V_y$ increases with L_x. In the quasi-2D case this ratio exceeds one only slightly in accordance with the experiments of Rouyer *et al.* [2].

D. Diffusion coefficients

We also studied the behavior of the particle (tracer) diffusion coefficient D defined by Eq. (3) using the memory expansion method [39]. We present D as a function of the volume fraction Φ in Figs. 10 and 11 in the periodic y and z directions, respectively. We have restricted to consider the system with $L_{\text{periodic}}=22.76$ and $L_x\leqslant 23.11$ in order to maintain reasonable accuracy to the results. In a dilute suspension, the qualitative behavior of D is different in the quasi-2D and 3D limits. While in the 3D limit D first increases due to increasing velocity fluctuations, in the quasi-2D geometry it is monotonically decreasing function over the whole range of Φ here. This result is expected due to the enhanced blocking in analogy to true 2D Brownian diffusion [40,41].

The different scaling of the velocity fluctuations with L_x is reflected in the size dependence of D_y and D_z, as can be seen in Figs. 10 and 11. While it is expected that D_z increases with L_x due to increasing ΔV_z, we find that D_y slightly *decreases* for larger values of L_x. To explain this behavior, it is useful to

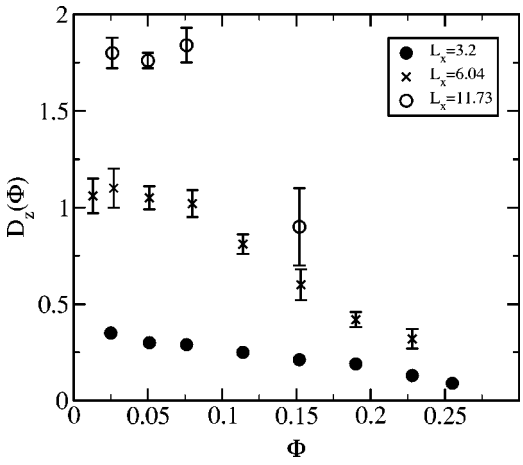

FIG. 11. The tracer diffusion coefficient in the z direction parallel to gravity.

distinguish between the scaling of ΔV and the autocorrelation time τ by using the relation $D=\Delta V^2\tau$. Our data for D_y thus suggest that τ_y decreases with L_x. Similar result has been obtained by Koch [25], who found that the autocorrelation time of the parallel component of the particle velocity decreases with the decreasing height to width ratio of a rectangular simulation box with periodic boundary conditions.

IV. SUMMARY AND CONCLUSIONS

To conclude, we have studied steady-state sedimentation with a fixed finite particle Reynolds number in a system periodic along the direction of gravity, but confined between two walls perpendicular to gravity. We have first considered the spatial distribution of particle number density in the container and found that a depletion region appears close to the walls for small volume fractions. This indicates that the particle-wall interaction dominates and thus particles interact weakly with each other. On the other hand, for large Φ there is an excess number of strongly interacting particles at the walls. The effect is most drastic in the dilute quasi-2D system where all particles are concentrated to the middle of the container interacting strongly with the walls.

Furthermore, we have shown that in a confined geometry, the average settling velocity obeys the RZ law but the exponent n changes as a function of the system width. In the quasi-2D system, the exponent has a value of $n=3.5$ while when the width increases n increases gradually to the 3D value of $n=5.5$. A qualitative explanation for the difference is that in a dilute system the particle-wall interaction is more prominent leading to a strong L_x dependence of the single particle velocities.

The velocity fluctuations in the quasi-2D system differ somewhat from the 3D case, which is most notably seen in the fact that the system size scaling cannot be extended to the case where $L_x=3.20$. The effect is most dramatic in the y direction, where ΔV_y does not depend on the wall spacing once $L_x \geqslant 6.04$ indicating that the increase in the single particle velocity does not play any significant role in the velocity fluctuations. The spatial asymmetry of the sedimentation box reveals the complicated interplay between the velocity fluctuations and the system size. In the direction parallel to the walls and perpendicular to the gravity (y) it is either L_y or L_z that controls the size of the velocity fluctuations, although we found no evidence of a finite-size scaling law. In the direction perpendicular to the walls (x), the controlling dimension is L_x until the spacing of the walls grows larger than the other dimensions L_y or L_z. Finally, in the direction parallel to gravity, ΔV_z is governed by L_x in all cases, with much weaker scaling with L_y and L_z. We also found that if L_x is much less than the periodic dimensions the velocity fluctuations scale with the system size, with fixed L_x/L_{periodic}, differently from the prediction of Caflisch and Luke [16]. The probable cause for this difference is the fixed particle Reynolds number changing the particle distributions as described below.

Finally, we have also studied the behavior of the tracer diffusion coefficients. Their dependence on the system size is less clear. The reason for this seems to be that τ and the corresponding velocity fluctuation scale different with system dimensions. Systematic study of the scaling was not feasible since it is computationally too demanding a task to try to calculate the diffusion coefficients for L_{periodic} larger than 22.76.

The inertial effects provided two clear difference to the $\text{Re}_p \ll 1$ case. First, wide depletion layers were formed in the vicinity of the walls, presumably increasing the effect of the intrinsic convection. Second, above each particle a region of reduced volume fraction is formed, which leads to a reduced spatial correlation length $R_{zz}(r)$.

In this work we systematically studied only one value of the particle Reynolds number. While the chosen $\text{Re}_p=0.5$ is large enough to ensure that inertial effects are visible, a systematic study of the strength of these effects is beyond the scope of the present work. With the data presented here, it is also unclear what the role of the container based Reynolds number is. According to the few cases studied we can, however, claim that the width of the depletion layer is a function of the Re_p rather than of the container based Reynolds number, although the exact form remains unclear. Most importantly, according to our additional simulations with Re_p varying between 0.1 and 1.0, we found that the spatial correlations of the particle velocities remain unchanged.

ACKNOWLEDGMENTS

This work has been supported in part by the Academy of Finland through its Center of Excellence Program. In addition, E.K. would like to thank the Finnish Cultural Foundation for support and J.M.L. gratefully acknowledges the support of the Väisälä Foundation. The code used for the numerical work has been developed at the Institute of Computer Applications, University of Stuttgart, Germany.

[1] S. Ramaswamy, Adv. Phys. **51**, 297 (2001).
[2] F. Rouyer, J. Martin, and D. Salin, Phys. Rev. Lett. **83**, 1058 (1999).
[3] M. L. Kurnaz and J. V. Maher, Phys. Rev. E **53**, 978 (1996).
[4] R. Barnea and J. Mizrahi, Chem. Eng. J. **5**, 171 (1973).
[5] H. Nicolai, B. Herzhaft, E. J. Hinch, L. Oger, and E. Guazzelli, Phys. Fluids **7**, 12 (1995).
[6] P. N. Segrè, E. Herbolzheimer, and P. M. Chaikin, Phys. Rev. Lett. **79**, 2574 (1997).
[7] G. K. Batchelor, J. Fluid Mech. **52**, 245 (1972).
[8] H. Hayakawa and K. Ichiki, Phys. Rev. E **51**, R3815 (1995).
[9] A. J. C. Ladd, Phys. Fluids **9**, 491 (1997).
[10] S. Schwarzer, Phys. Rev. E **52**, 6461 (1995).
[11] J. F. Richardson and W. N. Zaki, Trans. Inst. Chem. Eng. **32**, 35 (1954).
[12] U. Geigenmüller and P. Mazur, J. Stat. Phys. **53**, 137 (1988).
[13] D. Bruneau, F. Feuillebois, R. Anthore, and E. J. Hinch, Phys. Fluids **8**, 2236 (1996).
[14] D. Bruneau, F. Feuillebois, J. Bławzdziewicz, and R. Anthore, Phys. Fluids **10**, 55 (1998).
[15] S. Kim and S. J. Karrila, *Microhydrodynamics: Principles and Selected Applications* (Butterworth-Heinemann, Boston, 1991).
[16] R. E. Caflisch and J. H. C. Luke, Phys. Fluids **28**, 759 (1985).
[17] E. J. Hinch, in *Disorder and Mixing*, edited by E. Guyon, J.-P. Nadal, and Y. Pomeau (Kluwer Academic, Dordrecht, 1988).
[18] A. J. C. Ladd, Phys. Rev. Lett. **76**, 1392 (1996).
[19] H. Nicolai and E. Guazzelli, Phys. Fluids **7**, 3 (1995).
[20] J. H. C. Luke, Phys. Fluids **12**, 1619 (2000).
[21] A. J. C. Ladd, Phys. Rev. Lett. **88**, 048301 (2002).
[22] S. Y. Tee, P. J. Mucha, L. Cipelletti, S. Manley, M. P. Brenner, P. N. Segrè, and D. A. Weitz, Phys. Rev. Lett. **89**, 054501 (2002).
[23] D. L. Koch and E. S. G. Shaqfeh, J. Fluid Mech. **224**, 275 (1991).
[24] D. L. Koch, Phys. Fluids A **5**, 1141 (1993).
[25] D. L. Koch, Phys. Fluids **6**, 2894 (1994).
[26] M. P. Brenner, Phys. Fluids **11**, 754 (1999).
[27] N. Liron and S. Mochon, J. Eng. Math. **10**, 287 (1975).
[28] R. Gomer, Rep. Prog. Phys. **53**, 917 (1990).
[29] K. Höfler and S. Schwarzer, Phys. Rev. E **61**, 7146 (2000).
[30] L. D. Landau and E. M. Lifshitz, *Fluid Mechanics*, 1st ed. (Pergamon Press, Oxford, 1984).
[31] H. Hasimoto, J. Fluid Mech. **5**, 317 (1959).
[32] J. Happel and H. Brenner, *Low Reynolds Number Hydrodynamics* (Englewood Cliffs, New Jersey, 1965).
[33] Y. Peysson and E. Guazzelli, Phys. Fluids **10**, 44 (1998).
[34] P. Vasseur and R. G. Cox, J. Fluid Mech. **80**, 561 (1977).
[35] G. Bernard-Michel, A. Monavon, D. Lhuillier, D. Abdo, and H. Simon, Phys. Fluids **14**, 2339 (2002).
[36] E. Kuusela and T. Ala-Nissila, Phys. Rev. E **63**, 061505 (2001).
[37] J.-Z. Xue, E. Herbolzheimer, M. A. Rutgers, W. B. Russel, and P. M. Chaikin, Phys. Rev. Lett. **69**, 1715 (1992).
[38] P. N. Segrè, F. Liu, P. Umbanhower, and D. A. Weitz, Nature (London) **409**, 594 (2001).
[39] S. C. Ying, I. Vattulainen, J. Merikoski, T. Hjelt, and T. Ala-Nissila, Phys. Rev. B **58**, 2170 (1998).
[40] J. M. Lahtinen, T. Hjelt, T. Ala-Nissila, and Z. Chvoj, Phys. Rev. E **64**, 021204 (2001).
[41] J. M. Lahtinen, M. Mašín, T. Laurila, T. Ala-Nissila, and Z. Chvoj, J. Chem. Phys. **116**, 7666 (2002).